J Radioanal Nucl Chem (2012) 292:729–738
DOI 10.1007/s10967-011-1478-z

# Affinity and removal of radionuclides mixture from low-level liquid waste by synthetic ferrierites

**Ayman F. Seliman**

Received: 2 October 2011 / Published online: 21 October 2011


**Abstract** The affinity and removal efficiency of $^{137}Cs^{+}$, $^{133}Ba^{2+}$, $^{85}Sr^{2+}$ and $^{241}Am^{3+}$ mixture from aqueous solutions using two synthetic ferrierites HSZ 700KOA and 700KOD commercially used as a catalyst in oil industry were investigated. The uptake of metal ions as a function of different parameters has been studied using batch equilibrium technique. Kinetic curves showed that the equilibrium was mostly reached within 45 min for $Cs^{+}$ and $Ba^{2+}$ and revealed to be longer for $Sr^{2+}$ and $Am^{3+}$. Using Freundlich and Langmuir adsorption isotherms, the results showed that the affinity and adsorption capacity of 700KOA and 700KOD follow the order: $Cs^{+} > Ba^{2+} > Sr^{2+} > Am^{3+}$ with higher values for first material. Both adsorbents exhibited significant high capacity for $Cs^{+}$ relative to other cations giving $q_{max}$ 1.97 and 1.78 mmol $g^{-1}$ for 700KOA and 700KOD, respectively. All metals uptake found to be concentration dependant and independent of the pH over 2 to 10 range except $Am^{3+}$; this reveals that the adsorption mechanism is controlled mainly by pure ion exchange reaction for $Cs^{+}$, $Ba^{2+}$, $Sr^{2+}$ and by surface complexation mechanism for $Am^{3+}$. These simple nontoxic materials are recommended to be used for radioactive waste treatment especially fission product $^{137}Cs$ and activation product $^{133}Ba$.

**Keywords** Low-level liquid waste · Sorption · Synthetic ferrierites

A. F. Seliman (✉)
Department of Analytical Chemistry and Environmental Control, Hot Laboratory Center, Atomic Energy Authority, Inshas, Cairo, Egypt
e-mail: aymanseliman@yahoo.com

## Introduction

Nuclear industries and civil activities produce large volumes of liquid radioactive waste. Solidification and volume reduction of these liquid wastes are required to decrease the discharge and widespread distribution radionuclides into aquatic ecosystems and to obtain suitable waste forms for final disposal [1].

$^{137}Cs^{+}$, $^{133}Ba^{2+}$, $^{90}Sr^{2+}$ and $^{241}Am^{3+}$ are mixture of fission and activation products and may be found in low-level liquid waste of primary cooling water of nuclear power reactors [2]. $^{137}Cs$ is an important fission product and is of primary concern due to its high yield and relatively long physical half-life of 30.07 years. Health concern of $^{137}Cs$ comes mainly from its similarity to potassium that considers essential element in biological system and because of its hard gamma emission [3]. The radioactive isotope $^{90}Sr$, in particular, is an ecological and health concern due to its relatively long physical half-life of 28.79 years, high energy of $\beta$-decay and as a calcium analog, $^{90}Sr$ tends to accumulate in bone [4]. $^{241}Am$ poses a significant risk if ingested (swallowed) or inhaled. It can stay in the body for decades and continue to expose the surrounding tissues to both alpha and gamma radiation, increasing the risk of developing cancer. According to Canadian Nuclear Safety Commission, the maximum permissible limits of $^{137}Cs$ and $^{90}Sr$ in drinking water are 10 and 5 Bq $L^{-1}$, respectively. The maximum contaminant level established for the same elements by the US-Environmental Protection Agency is 7.41 Bq $L^{-1}$ for $^{137}Cs$ and 0.30 Bq $L^{-1}$ for $^{90}Sr$.

Over the few decades, several conventional treatment technologies have been considered for the treatment and removal of radionuclides from aqueous solutions. These include evaporation, precipitation, ion exchange,

adsorption and membrane. However, some of these processes have significant disadvantages such as incomplete metal removal, particularly at low concentrations, low thermal and radiological stability. Also, precipitation, by adjusting the pH value, is not selective and produces large quantities of solid sludge for disposal [5]. Relative to these treatment technologies, inorganic ion exchangers and sorbent materials have been successfully tested for treating several types of liquid waste, replacing older techniques.

Several researchers have studied the separation efficiency and removal performance of radionuclides by different inorganic exchangers. Roy et al. [6] developed and characterized new zirconium vanadate exchanger for separation $^{133}$Ba from $^{134}$Cs at tracer level using 0.1 M ammonium chloride. Removal of Sr(II) ions from aqueous solutions by potassium tetratitanate whisker (PTW) and sodium trititanate whisker (STW) was studied by the batch sorption system. Langmuir model represented a better fit to the experimental data than Freundlich isotherm model, and the monolayer sorption capacity is 1.01 and 0.09 mmol $g^{-1}$ for PTW and STW, respectively [7].

Marinin and Brown [8] investigated different sorbents selectivity to strontium in the presence of calcium and kinetic measurements of strontium removal in low-level liquid radioactive waste (LLRW). Modifications of Amberlite and Duolite ion-exchange resins (Rohm and Haas, USA) and new synthetic crystalline materials silicotitanate IE-911 (UOP, USA) and sodium titanate (Allied Signal, USA) showed the highest distribution coefficients of strontium ($K_d \sim 2 \times 10^4$–$4 \times 10^5$ mL $g^{-1}$). Adsorption of barium was evaluated by natural and synthetic adsorbents clinoptilolite and montmorillonite [9], hydrous bismuth oxide [10], nanoparticles of zero-valent iron [11] and phillipsite-rich tuffs [12].

Although, there are many studies in literatures about removing radionuclides using inorganic exchangers, but using laboratory scale quantity sometimes have difficulties to be reproduced with the same characteristics. Other materials contain toxic elements [13–15]. So, the need for investigating the commercially available products with specific properties and nontoxic constituents looks essential to have well known materials for hazardous waste treatment. Therefore, the current research aims to investigate and quantify the efficiency of two synthetic ferrierites 700KOA and 700KOD generally used as a catalyst in oil industry to adsorb and remove mixture of four radionuclides with different oxidation states and ionic radii $^{137}Cs^{+}$, $^{133}Ba^{2+}$, $^{85}Sr^{2+}$ and $^{241}Am^{3+}$ from a simulated low-level radioactive liquid waste and to compare their retention properties with other materials conventionally used in aqueous waste treatment.

## Experimental

### Materials and reagents

Synthetic Ferrierites 700KOA and 700KOD samples are commercial products from Tosoh Corporation, Japan. 700KOA is in white powder form with particle size <54 μm and used as received from the supplier. 700KOD came in brownish Pellets form that was crushed, grounded and sieved to mesh size 75–100 μm. All chemicals and reagents used for experiments and analyses were of analytical grade and were used without further purification. Stock solutions of 4000 mg $L^{-1}$ Cs(I), Sr(II) and Ba(II) were prepared from CsCl, $Sr(NO_3)_2$ and $Ba(NO_3)_2$ salts in bidistilled water, while 1000 mg $L^{-1}$ Eu(III) used as an analogue for $^{241}$Am was prepared from $Eu_2O_3$ in 2% $HNO_3$. 1 M $NaNO_3$ and $NaClO_4$ were prepared from their salts to be used as a background solution in adsorption and titration experiments, respectively. The radioactive tracers used in all experiments were obtained from Amersham International (UK).

### Characterization

Diffraction data of the materials were collected with a Philips PW1710 powder X-ray diffractometer (XRD) with Cu $K_\alpha$ radiation (1.54 Å) operating at 40 kV and 50 mA. The water contents were determined in thermogravimetric analyses (TGA) that were carried out on a Mettler-Toledo TGA850 unit, at a heating rate of 10 °C $min^{-1}$ under a nitrogen atmosphere. The surface morphology was examined by Hitachi S-4800 field emission scanning electron microscope (FESEM). Coarse elemental analyses were carried out from energy-dispersive X-ray spectroscopy (EDX) spectra recorded by Oxford INCA 350 microanalysis system connected to a Hitachi S-4800 FESEM and using INCA suite version 4.05 software. Four punctual analyses were carried out for each synthetic ferrierite sample. Powdered samples with surface carbon coating were used. Potentiometric titration of the magnetically stirred aqueous synthetic ferrerites suspensions (5 g $L^{-1}$) were carried out under nitrogen atmosphere and at 22 °C, on a Metrohm 665 titrator equipped with a pH electrode. The point of zero charge (PZC) was determined for two different ionic strength 0.1 and 0.25 M using $NaClO_4$ as background solutions.

### Batch adsorption studies

The equilibrium sorption experiments of $^{137}Cs^{+}$, $^{133}Ba^{2+}$, $^{85}Sr^{2+}$ and $^{241}Am^{3+}$ on synthetic ferrierites 700KOA and 700KOD were carried out at constant temperature (22 ± 2 °C) and ionic strength (0.01 M) by $NaNO_3$ in 15 mL polypropylene centrifuge tube with screw cap. All tests were

conducted using 0.10 g of adsorbent with 10 mL of solutions containing a mixture of the radionuclides. The suspensions were shaken in end-over-end mixer. In all cases, the sorbents were removed from the solutions by centrifugation for 20 min at 4000 rpm using Thermo Scientific MR23i Centrifuge. The solutions were filtered with 0.45 μm Whatman membrane filter. Aliquots (5 mL) of solution before and after the experiments were quantified for $^{137}$Cs, $^{133}$Ba, $^{85}$Sr and $^{241}$Am mixture using standard high purity germanium (HPGe) gamma-ray spectrometric system.

To study the effect of pH on the adsorption behavior of radionuclides, the solutions pH from 2.0 to 10.0 was adjusted by additions of $HNO_3$ or NaOH before adding 700KOA or 700KOD adsorbent. All pH experiments were performed with solution of initial concentrations 20 mg $L^{-1}$ of $Cs^+$, $Ba^{2+}$, $Sr^{2+}$ and 5 mg $L^{-1}$ of $Am^{3+}$($Eu^{+3}$). The pH values at the beginning and the end of experiments were measured with an Orion 3-star plus pH meter with a BNC waterproof electrode after overnight mixing. The same experiments were repeated to study the effect of shaking time from 0.5 to 1200 min.

To measure adsorbents capacity for each radionuclide, the effect of radionuclides concentration at constant temperature and pH (4.5) was investigated. The initial concentration varied from 20 to 600 mg $L^{-1}$ for $Ba^{2+}$ and $Sr^{2+}$; 5 to 250 mg $L^{-1}$ for $Am^{3+}$($Eu^{3+}$) and from 240 to 1600 mg $L^{-1}$ (4 successive loading) for $Cs^+$. Suspensions were shaken for 4 h, which had been found sufficient to ensure equilibration.

### Aqueous speciation and data regression

Visual MINTEQ code Ver. 2.6 [16] was used to calculate speciation distribution of the investigated radionuclides in the liquid phase at different pH values. Initial thermodynamic constants of $Cs^+$, $Ba^{2+}$, $Sr^{2+}$ and $Am^{3+}$ ions with inorganic ligands are the ones from the MINTEQ database at 25 °C and ionic strength = 0 mol $L^{-1}$. The species distribution of $Cs^+$, $Ba^{2+}$, $Sr^{2+}$ and $Am^{3+}$ were calculated at the same experimental conditions.

For data regression, ion exchange behavior of different concentrations of each metal onto 700KOA and 700KOD synthetic ferrierite was represented by Langmuir and Freundlich isotherm models. The models adjustable parameters were optimized by nonlinear least square fitting regression of all adsorption data using the solver add-in tool with Microsoft Excel.

## Results and discussion

### Adsorbents characterization

The XRD spectra of the 700KOA and 700KOD synthetic ferrierites are given in Fig. 1. According to different electronic databases, included in the X-ray diffractometer, the result indicates that the adsorbents used in this study are pure aluminum silicate (ferrierite). The structure of both materials is crystal and looks very similar, the exception is two small peaks for 700KOD at 19.5, 20.5 and peaks intensity difference in the two-theta interval 25–27.5 for the two materials. Other metals content was demonstrated by measuring the coarse elemental composition by energy-dispersive X-ray spectroscopy (EDX), Table 1. The data revealed that the two materials contain K and Na ions as cations type. The $SiO_2/Al_2O_3$ ratio found to be 12.4 and 12.0 for 700KOA and 700KOD, respectively and these are almost the same as reported by the supplier. SEM micrographs revealed that both adsorbents have different morphology, where 700KOA consists of homogeneous small particles with smooth surface relative irregular powder form for 700KOD as shown in Fig. 2. The water content was measured using TGA for 700KOA and 700KOD. The results show that 700KOA has higher water content with 9.6% comparing to 700KOD with 8.7%.

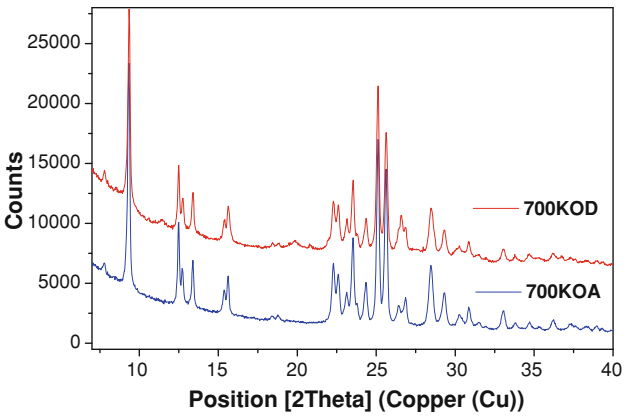


**Fig. 1** XRD patterns of 700KOA and 700KOD synthetic ferrierite

**Table 1** Chemical composition of synthetic ferrierites using EDX analysis

| Element (wt%) | 700KOA | 700KOD |
|---|---|---|
| $SiO_2$ | 81.51 | 81.58 |
| $Al_2O_3$ | 11.15 | 11.35 |
| $K_2O$ | 5.66 | 5.06 |
| $Na_2O$ | 1.70 | 1.50 |
| $SiO_2/Al_2O_3$ (mol/mol)[a] | 12.40 | 12.20 |
| Cation type | K, Na | K, Na |
| Empirical formula | $K_2O{\cdot}Al_2O_3{\cdot}mSiO_2{\cdot}nH_2O$ | $K_2O{\cdot}Al_2O_3{\cdot}mSiO_2{\cdot}nH_2O$ |
| Mean particle size (μm) | <54 | 75–100 |

[a] The $SiO_2/Al_2O_3$ ratio reported by Tosoh Corporation, Japan is 12.20 for two materials

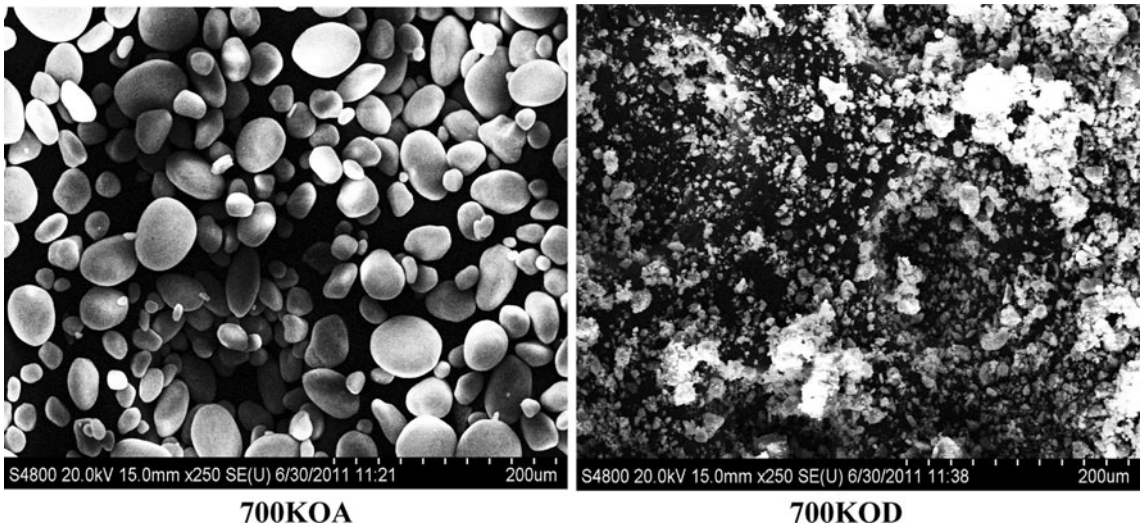


**Fig. 2** SEM micrograph of 700KOA and 700KOD synthetic ferrierite

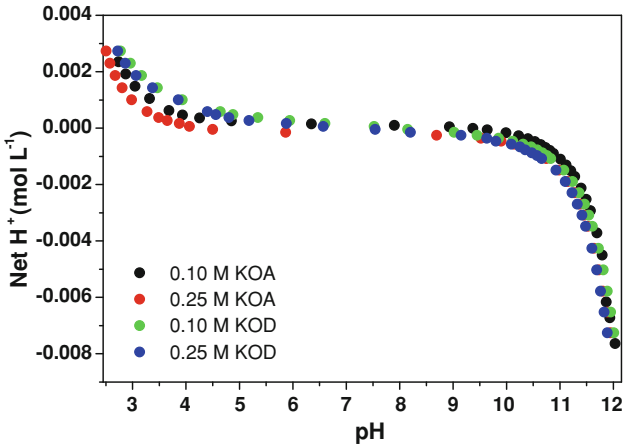


**Fig. 3** Potentiometric titration curves of 700KOA and 700KOD synthetic ferrierites as a function of pH at different ionic strengths using $NaClO_4$ as a background electrolyte

Potentiometric titration curves of 700KOA and 700KOD as a function of pH versus the net of proton concentration (mol $L^{-1}$) at different ionic strengths are presented in Fig. 3. The PZC found to be 9.0–9.3 and 7.0–7.75 for 700KOA and 700KOD, respectively. Although the two investigated materials have similar $SiO_2/Al_2O_3$ ratio, 700KOD gives lower PZC values that may be due to some higher permanent surface charges result from small difference in crystal structure [17].

## Effect of pH

The results of the uptake experiments of $Cs^+$, $Ba^{2+}$, $Sr^{2+}$ and $Am^{3+}$ as a function of solution pH values ranging from 2 to 10 by 700KOA and 700KOD synthetic ferrierites are shown in Fig. 4. The general trend of four elements on both materials shows that the uptake percentage of $Cs^+$, $Ba^{2+}$ and $Sr^{2+}$ does not change with the change in solution pH except $Am^{3+}$, where small uptake was observed at low pH. This means that the adsorption of $Cs^+$, $Ba^{2+}$ and $Sr^{2+}$ is highly independent on the surface characteristics of the adsorbents at various pH values but may be correlated to the permanent surface negative charge of synthetic ferrierites crystals and the chemical species forms of these ions in the aqueous phase. Aqueous speciation distribution of radionuclides mixture was calculated and represented in Fig. 5. The results show that the free metal ions $Cs^+$, $Ba^{2+}$ and $Sr^{2+}$ are the predominant species at the pH range 2.5–11 with mean total percent 99.10, 96.62 and 96.27, respectively. The speciation of Am(III) indicate that uncomplexed ion $Am^{3+}$ is the predominant aqueous species for moderately and highly acidic conditions with >90% of total concentration. At near neutral and alkaline pH conditions, Am-hydroxide complexes start to dominate the aqueous phase. At pH 7, the $Am(OH)^{2+}$ became the major species with 60%, while at pH 9.5, $Am(OH)_2^+$ became the predominant species within total percent close to 98% of total americium. The formation of $Am(OH)_3(aq)$ species starts to grow after pH 10.

Based on this calculation, the adsorption mechanism of the radionuclides onto 700KOA and 700KOD is mainly pure ion exchange reactions for $Cs^+$, $Ba^{2+}$ and $Sr^{2+}$ and looks to be surface complexation reaction for $Am^{3+}$. This conclusion is supported by the structural characteristics of aluminum silicates that have unique ion exchange properties. Theses properties come from their framework structure which enclosing cavities occupied by cations to compensate for the imbalance created by the substitution of $Al^{3+}$ for $Si^{4+}$ in the basic structure [18].

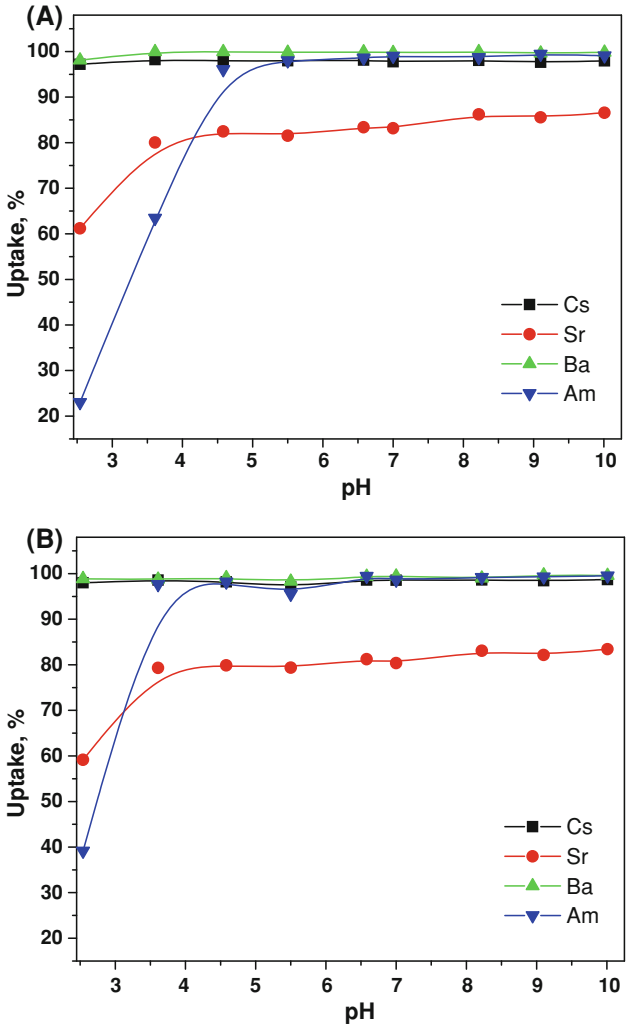


**Fig. 4** The uptake of $Cs^{+}$, $Ba^{2+}$, $Sr^{2+}$ and $Am^{3+}$ on synthetic ferrierites 700KOA (**a**) and 700KOD (**b**) as a function of solution pH in 0.01 M $NaNO_3$

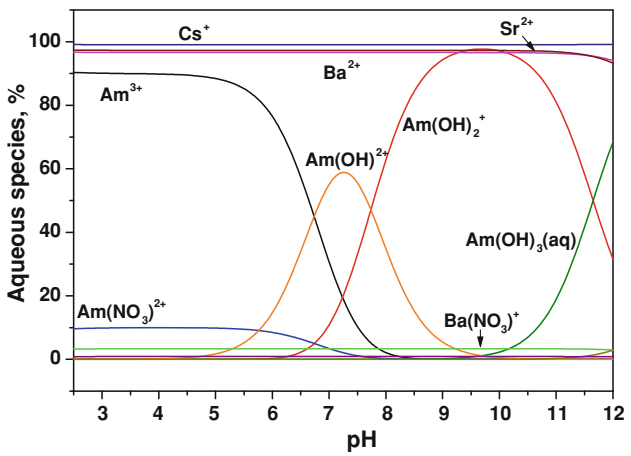


**Fig. 5** Predicted aqueous speciation of Cs(I), Ba(II), Sr(II) and Am(III) as a function of pH in 0.01 M $NaNO_3$

## Adsorption kinetic studies

The results of the kinetic experiments of the ion exchange reaction using 20 ppm of $Cs^{+}$, $Ba^{2+}$, $Sr^{2+}$ and $Am^{3+}$ from aqueous solutions mixture onto the synthetic ferrierite as a function of contact time were presented in Fig. 6. The data show that the adsorption is a heterogeneous process for $Ba^{2+}$, $Sr^{2+}$ and $Am^{3+}$ with an initial rapid adsorption rate followed by a slower uptake. At the beginning, the adsorption sites are available and the metals ions interact easily with the sites and hence a higher rate of adsorption is reported. A homogeneous adsorption process is observed for $Cs^{+}$ where the uptake is fast and did not change within the whole time range. This means that the number of sites available for $Cs^{+}$ is significantly higher than the used concentration.

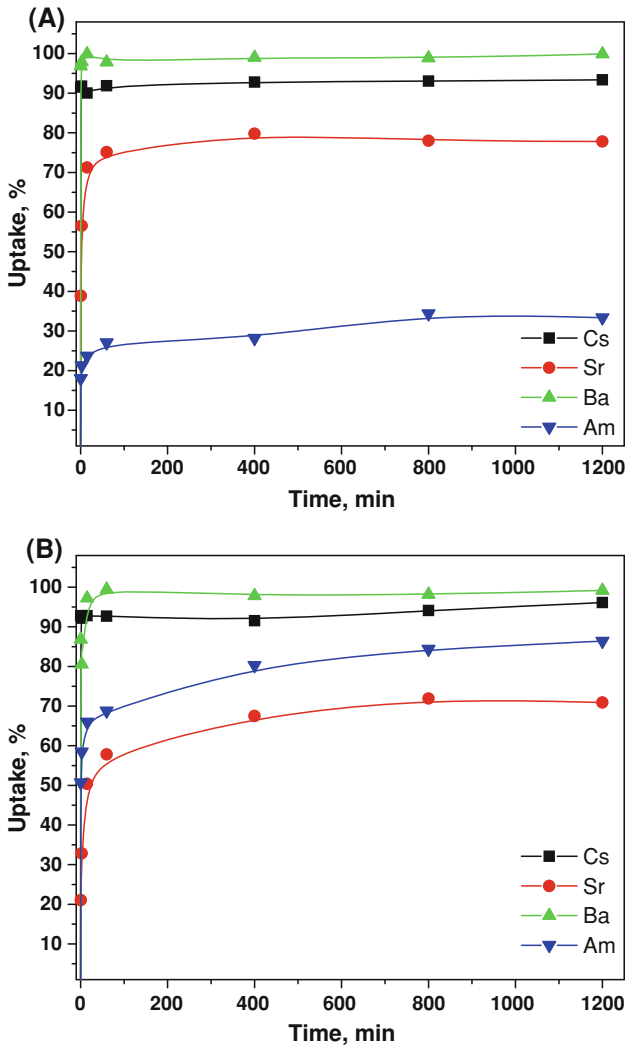


**Fig. 6** The uptake of $Cs^{+}$, $Ba^{2+}$, $Sr^{2+}$ and $Am^{3+}$ on synthetic ferrierites 700KOA (**a**) and 700KOD (**b**) as a function of shaking time in 0.01 M $NaNO_3$

At the first 45 min near 90, 99, 75 and 30% of $Cs^{+}$, $Ba^{2+}$, $Sr^{2+}$ and $Am^{3+}$, respectively, are adsorbed onto 700KOA. A higher adsorption percentage of $Am^{3+}$ and a lower percentage of $Sr^{2+}$ were reported for 700KOD. In all cases, the rest of radionuclides concentrations are sorbed during 800 min. The slower adsorption especially for $Sr^{2+}$ and $Am^{3+}$ during the second stage may be attributed to (1) the few number of adsorption sites selective for these ions, (2) ion exchange process take place in micropores inside separate adsorbent microcrystals [19]. According to these results, 45 min contact time is considered sufficient for the $Cs^{+}$ and $Ba^{2+}$ adsorption, while 100 min are almost enough for $Sr^{+}$ and $Am^{3+}$ uptake by both materials. Chavez et al. [9] reported a similar kinetic behavior for $Ba^{2+}$ adsorption by Ca-exchange clinoptilolite tuff and montmorillonite clay where, an initial fast intake of $Ba^{2+}$ within 60 min followed by a much slower adsorption that is essentially completed and attained equilibrium after 10 h of contact. 400 min are used as a contact time for all the rest of the batch experiments.

### *Adsorption kinetic modeling*

Two different models were used to investigate the rate of $Cs^{+}$, $Ba^{2+}$, $Sr^{2+}$ and $Am^{3+}$ adsorption by synthetic ferrierites. The pseudo-first-order found to be not fit enough to represent the kinetic data, so, the data was modeled using the pseudo-second-order equation. This model is based on the sorption capacity of the solid phase and its linear form is written as [20]:

$$\frac{t}{q_t} = \frac{1}{k_2 q_e^2} + \frac{1}{q_e} t \qquad (1)$$

where $k_2$ (g mmol$^{-1}$ min$^{-1}$) is the rate constant, $q_e$ (mmol g$^{-1}$) the amount of radionuclide adsorbed at equilibrium and $q_t$ (mmol g$^{-1}$) is the amount adsorbed at any time $t$ (min).

The fitting parameters of pseudo-second-order equation to the experimental data are reported in Table 2. Based on the correlation coefficient of linear regression analysis, pseudo-second-order found to give excellent fit to all results with $r^2$ value ranging from 0.998 in the case of $Am^{3+}$/700KOA system to 0.999 for other systems. The rate constant ($k_2$) values found to obey the order: $Cs^{+} > Ba^{2+} > Sr^{2+} > Am^{3+}$ on 700KOA, while follow the sequence: $Ba^{2+} > Cs^{+} > Am^{3+} > Sr^{2+}$ on 700KOD.

## Adsorption isotherms

### *The radionuclides distribution coefficient ($K_d$)*

The adsorption of $Cs^{+}$, $Ba^{2+}$, $Sr^{2+}$ and $Am^{3+}$ onto synthetic ferrierites as a function of their concentrations was studied at 25 °C while, keeping all other parameters constant. The $K_d$ value was calculated as a function of metal ion concentrations from 20 to 600 ppm for $Cs^{+}$, $Ba^{2+}$ and $Sr^{2+}$ and from 5 to 250 ppm for $Am^{3+}$ using the following equation:

$$K_d = \frac{(C_0 - C_e)}{C_e} x \frac{V}{m} \text{ mL/g}, \qquad (2)$$

where $C_o$ and $C_e$ are the initial and equilibrium aqueous metal concentration (mg L$^{-1}$), respectively. $V$ is the solution volume (mL) and $m$ is the weight of the adsorbent (g).

Because the uptake behavior of $Am^{3+}$ was studied at lower concentration range and found to be different and generally low relative to other radionuclides, only the $K_d$ values of $Cs^{+}$, $Ba^{2+}$ and $Sr^{2+}$ as a function of metal ions concentration (20–600 ppm) were reported in Table 3. The $K_d$ values generally increase with the decreasing concentration of radionuclides. These results indicate that energetically less favorable sites become involved with increasing metal concentration in the aqueous solution. This behavior may be attributed to the ion-exchange mechanism, where metal ions had to move through the pores of the ferrerites mass and channels of the lattice to replace the exchangeable $Na^{+}$ and $K^{+}$ cations. Diffusion was easy and faster through the pores and was retarded when the ions moved through the smaller diameter channels [21]. This explain why the metals uptake become high at low concentration, where the competition on the exchangeable sites on the wide pores is at its minimum

**Table 2** The kinetic pseudo-second order fitting parameters

| Element | 700KOA | | | 700KOD | | |
|---|---|---|---|---|---|---|
| | $q_e$ | $k_2$ | $r^2$ | $q_e$ | $k_2$ | $r^2$ |
| $Cs^{+}$ | 0.0277 | 198.91 | 0.999 | 0.0281 | 14.67 | 0.999 |
| $Ba^{2+}$ | 0.0284 | 62.67 | 0.999 | 0.0284 | 95.89 | 0.999 |
| $Sr^{2+}$ | 0.0356 | 25.84 | 0.999 | 0.0319 | 5.44 | 0.999 |
| $Am^{3+}$ | 0.0087 | 10.61 | 0.998 | 0.0222 | 6.46 | 0.999 |

$q_e$ is the amount of metal ions adsorbed at equilibrium, mmol g$^{-1}$

$k_2$ is the pseudo-second order rate constant, g mmol$^{-1}$ min$^{-1}$

**Table 3** The $K_d$ values of $^{137}Cs$, $^{85}Sr$ and $^{133}Ba$ on synthetic ferrierites 700KOA and 700KOD as a function of metals concentration

| Conc., ppm | Radionuclide $K_d$ (mL $g^{-1}$) | | |
|---|---|---|---|
| | $^{137}Cs$ | $^{85}Sr$ | $^{133}Ba$ |
| 700KOA | | | |
| 20 | 26595 | 7663 | 602935 |
| 40 | 16204 | 1968 | 85326 |
| 80 | 9290 | 410 | 46765 |
| 120 | 6258 | 183 | 13044 |
| 240 | 2912 | 51 | 1442 |
| 480 | 1632 | 29 | 306 |
| 600 | 1276 | 18 | 189 |
| 700KOD | | | |
| 20 | 31781 | 5334 | 573965 |
| 40 | 25666 | 1965 | 48678 |
| 80 | 7325 | 392 | 7789 |
| 120 | 9447 | 193 | 7244 |
| 240 | 4572 | 64 | 1034 |
| 480 | 1889 | 23 | 197 |
| 600 | 1393 | 23 | 132 |

value relative to the difficult ion exchange reaction on sites within narrow lattice channels.

The $K_d$ values generally follow the order of $Ba^{2+} > Cs^+ > Sr^{2+}$ for 700KOA and 700KOD adsorbents at lower concentrations. The distribution coefficient of $Ba^{2+}$ is higher than $Cs^+$ until concentration 120 ppm, after that the $K_d$ values of $Cs^+$ became higher than $Ba^{2+}$. This trend indicates that the number of sites selective for $Cs^+$ is significantly higher than that is selective for $Ba^{2+}$. Behrens and Clearfield [22] investigated the affinity of sodium and potassium titanosilicate towards $10^{-3}$ M $Cs^+$, $Sr^{2+}$ and $Ba^{2+}$ without any added electrolyte. For potassium titanosilicate, the selectivity sequence follows the order $Sr^{2+} > Cs^+ > Ba^{2+}$ with $K_d$ values 51270, 3500 and 1960 mL $g^{-1}$, respectively. While the sodium phase yielded totally different $K_d$ values around 51360 mL $g^{-1}$ for $Cs^+$, 8800 mL $g^{-1}$ for $Ba^{2+}$ and 6490 mL $g^{-1}$ for $Sr^{2+}$.

The distribution coefficient of $Am^{3+}$ was calculated at concentration range 5–250 ppm and the results revealed that the $K_d$ of $Am^{3+}$ using 700KOD is higher than using 700KOA. This may be due to the higher number of permanent surface charges estimated from potentiometric titration for 700KOD ferrierite crystals and to the number of pore size fit to $Am^{3+}$ ionic radii in the same material.

*Adsorbents affinity and capacity*

The results of simultaneous adsorption of $Cs^+$, $Ba^{2+}$, $Sr^{2+}$ and $Am^{3+}$ by 700KOA and 700KOD synthetic ferrierites were fitted by non-linear equations of both Langmuir and Freundlich isotherm models as shown in Fig. 7 and Table 4. The uptake of radionuclides increases as the initial concentrations increase in almost all cases. Freundlich model gives a better fit with a mean $r^2 = 0.963 \pm 0.052$ compared to the Langmuir adsorption isotherm with a mean $r^2 = 0.928 \pm 0.075$.

Freundlich adsorption isotherm is usually used to fit experimental data over a wide range of concentrations by the following equation:

$$q_e = K_f C_e^{1/n} \tag{3}$$

where $K_f$ and $1/n$ are empirical constants. The magnitude of the exponent $1/n$ gives an indication of the favorability of adsorption. Values of $n$, where $n > 1$ represent favorable adsorption condition.

The good fit with this model suggesting that the two synthetic ferrierites contained heterogeneous surface characteristics with sites of varied affinities [23]. According to the distribution coefficients estimated from the used Freundlich model, the adsorption affinity of radionuclides follow the sequence: $Cs^+ > Ba^{2+} > Sr^{2+} > Am^{3+}$ on 700KOA and 700KOD. Comparison the affinity of both sorbents to radionuclides reveals that 700KOA has a higher affinity for $Cs^+$, $Ba^{2+}$ and $Sr^{2+}$ with $K_f$ values 3.67, 0.81 and 0.45, respectively. But 700KOD has a $K_f$ value of 0.17 for $Am^{3+}$ relative to 0.10 in the case of 700KOA. The value of $n$ in most cases falling between 2 and 10 indicates favorable adsorption for radionuclides on both adsorbents. This behavior is mainly due to the high affinity of $Cs^+$ and $Ba^{2+}$ for the available surface sites. The sites are considered limited for $Ba^{2+}$ relative to that for $Cs^+$.

Langmuir equation was used to calculate the maximum capacity ($q_m$) of the investigated radionuclides from the following expression:

$$q_e = q_m \frac{bC_e}{1 + bC_e} \tag{4}$$

where $C_e$ is the equilibrium aqueous metal ions concentration (mmol $L^{-1}$), $q_e$ the amount of metal ions adsorbed per gram of adsorbent at equilibrium (mmol $L^{-1}$), $q_m$ and $b$ are the Langmuir constants related to the maximum adsorption capacity and energy of adsorption, respectively.

The maximum capacity ($q_m$) estimated from Langmuir isotherm revealed the same affinity sequence reported from Freundlich model. This sequence is $Cs^+ > Ba^{2+} > Sr^{2+} > Am^{3+}$ with maximum sorption capacity 1.968, 0.275, 0.094 and 0.019 mmol $g^{-1}$, respectively, on 700KOA. Using 700KOD, the $q_m$ is calculated to be 1.784, 0.210, 0.057 and 0.052 mmol $g^{-1}$ for $Cs^+ > Ba^{2+} > Sr^{2+} > Am^{3+}$, respectively. This sequences obeys the same order of ionic radii for the investigated radionuclides $Cs^+$ (181 pm), $Ba^{2+}$ (149 pm), $Sr^{2+}$ (132 pm) and $Am^{3+}$ (111.5 pm).

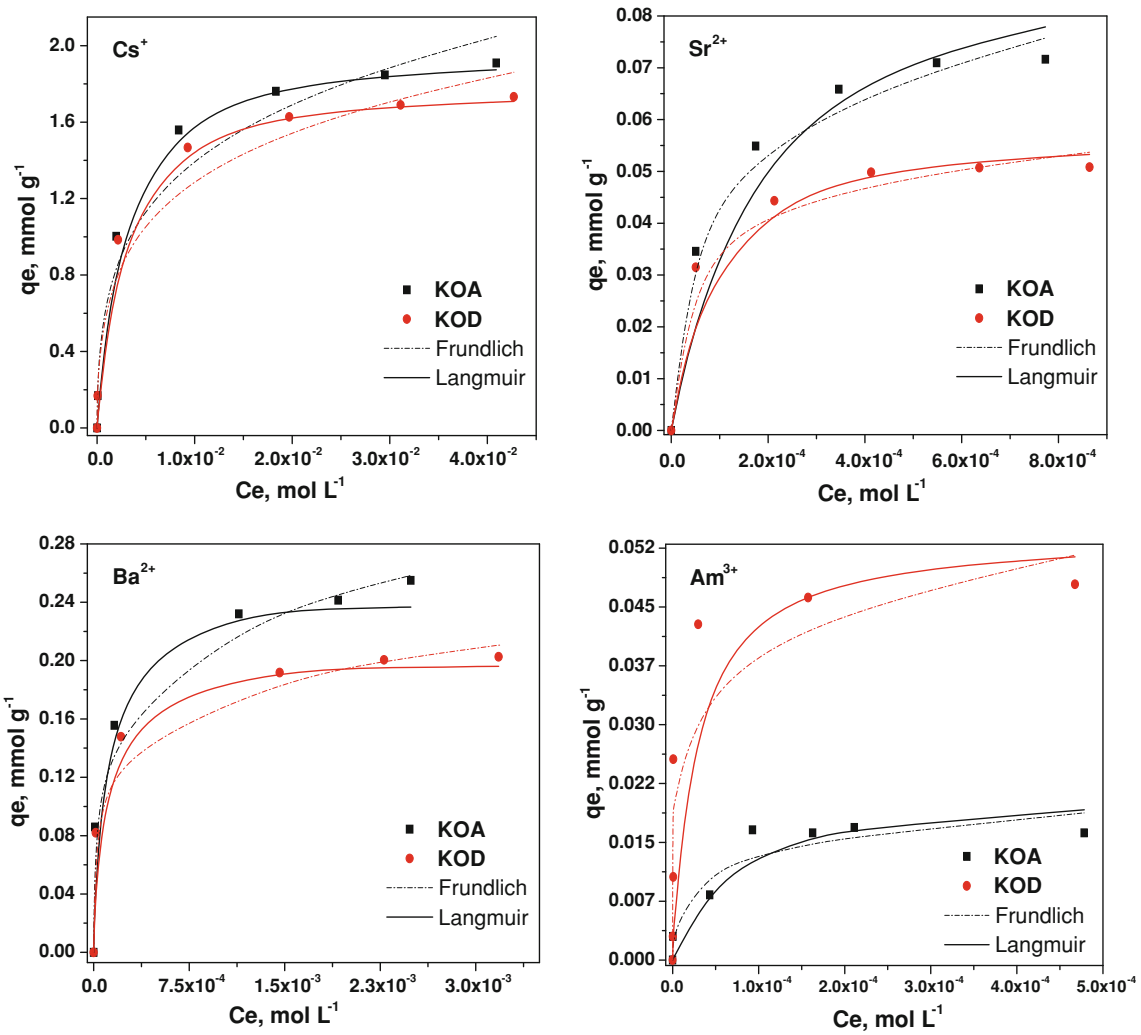


**Fig. 7** Experimental and modeled adsorption isotherms of of $Cs^{+}$, $Ba^{2+}$, $Sr^{2+}$ and $Am^{3+}$ on 700KOA and 700KOD synthetic ferrierites using Freundlich and Langmuir equation. (pH = 4.5; V/m = 100; 0.01 M $NaNO_3$)

**Table 4** Adjustable isotherm parameters and correlation coefficients calculated using experimental data

| Element | Freundlich | | | Langmuir | | |
|---|---|---|---|---|---|---|
| | $K_f$ | $n$ | $r^2$ | $b$ | $q_m$ | $r^2$ |
| 700KOA | | | | | | |
| $Cs^{+}$ | 3.67 | 5.17 | 0.989 | 507 | 1.968 | 0.999 |
| $Ba^{2+}$ | 0.81 | 5.25 | 0.997 | 5600 | 0.275 | 0.887 |
| $Sr^{2+}$ | 0.45 | 4.04 | 0.986 | 6400 | 0.094 | 0.946 |
| $Am^{3+}$ | 0.10 | 4.61 | 0.900 | 25800 | 0.019 | 0.926 |
| 700KOD | | | | | | |
| $Cs^{+}$ | 3.12 | 5.71 | 0.990 | 555 | 1.784 | 0.999 |
| $Ba^{2+}$ | 0.52 | 6.33 | 0.991 | 10602 | 0.210 | 0.920 |
| $Sr^{2+}$ | 0.18 | 5.81 | 0.989 | 15400 | 0.057 | 0.976 |
| $Am^{3+}$ | 0.17 | 6.41 | 0.860 | 80433 | 0.052 | 0.771 |

Isotherm parameters correspond to uptake, $q_e$, in mmol per gram and concentration, $C_e$, in mole per liter: $K_f$ ($M^{(1-n)}$ $L^n$ $g^{-1}$): $n$ is dimensionless; $q_m$ (mmol $g^{-1}$); $b$ (L $M^{-1}$)

The difference in adsorption capacity of the synthetic ferrierites for the radionuclides may be due to number of factors which include ionic radii, hydration diameters, hydration enthalpies, the charge to radius ratio ($Z/r$) and solubility of the cations as discussed in details by Motsi et al. [24]. The low adsorption capacity and relatively poor removal of $Am^{3+}$ by 700KOA and 700KOD synthetic ferrierites is probably caused by the few lattice channels number of pore size fit to the ionic radius of americium ions relative to that are fit to other metals ions. This may be also the same reason of the high 700KOA capacity reported for $Cs^{+}$, $Ba^{2+}$ and $Sr^{2+}$ relative to 700KOD.

The adsorption capacities ($q_m$) of different adsorbents for adsorption of Cs(I), Sr(II), Ba(II) and Am(III) ions are compared in Table 5. It may be seen that $q_m$ values differ widely for different adsorbents. Comparison of $q_m$ values shows that 700KOA and 700KOD adsorbent have high and moderate adsorption capacity for Cs(I) and Ba(II),

**Table 5** Adsorption capacity of various adsorbents for $Cs^{+}$, $Sr^{2+}$, $Ba^{2+}$ and $Am^{3+}$

| Element | Adsorbent | $q_m$ (mmol $g^{-1}$) | References |
|---|---|---|---|
| $Cs^{+}$ | 700KOA | 1.968 | This work |
| | 700KOD | 1.784 | This work |
| | IONSIV IE-911; TAM-5[a] | 0.519; 0.617 | [25] |
| | AMP-CaALG[b] | 0.688 | [26] |
| | Montmorillonite | 0.706 | [27] |
| | Zeolites[c] | 1.27-2.07 | [28] |
| $Sr^{2+}$ | 700KOA | 0.094 | This work |
| | 700KOD | 0.057 | This work |
| | Moss | 0.160-0.434 | [29] |
| | Dolomite | 0.013 | [30] |
| | SMP-PAA[d] | 0.26 | [31] |
| | Hydroxyapatite | 0.582 | [32] |
| $Ba^{2+}$ | 700KOA | 0.275 | This work |
| | 700KOD | 0.21 | This work |
| | Zero valent-iron | 0.157 | [11] |
| | Zeolite–Montmorillonite | 0.111 | [9] |
| | Clinoptilolite | 0.131-0.655 | [33] |
| | Dolomite | 0.029 | [30] |
| $Am^{3+}$ | 700KOA | 0.019 | This work |
| | 700KOD | 0.052 | This work |
| | Calcium alginate | 0.088 | [34] |
| | Dried tannin | 0.007 | [35] |

[a] Crystalline silicotitanate inorganic ion exchanger, IONSIV IE-911, and its parent precursor, TAM-5

[b] Ammonium molybdophosphate–calcium alginate composite

[c] Zeolites, natural clinoptilolite, natural chabazite, natural mordenite and synthetic mordenite

[d] SMP-PAA, stannic molybdophosphate (SMP) and poly-acrylamide (PAA)

respectively, relative to other products. General small capacities are reported for Sr(II) and Am(III) adsorption from aqueous solutions.

## Conclusion

The results from the present study show that the adsorption processes of $Cs^{+}$, $Ba^{2+}$, $Sr^{2+}$ and $Am^{3+}$ on two different synthetic ferrierites 700KOA and 700KOD are dependent on initial metals concentration and contact time. The uptake of $Cs^{+}$ and $Ba^{2+}$, did not affect by changing the solution pH values between 2.5 and 10, while the adsorption of $Sr^{2+}$ and $Am^{3+}$ revealed low adsorption at $pH < 4.0$. This indicates that pure ion exchange process is the main mechanism responsible for $Cs^{+}$ and $Ba^{2+}$ adsorption and mixed or surface complexation reactions control the behavior of $Sr^{2+}$ and $Am^{3+}$ ions.

The Freundlich and Langmuir isotherms were applied to the sorption data. The adsorption affinity and maximum capacity found to follow the sequence: $Cs^{+} > Ba^{2+} > Sr^{2+} > Am^{3+}$ with higher values for 700KOA, the exception is the higher $Am^{3+}$ capacity reported for 700KOD. Both materials found to be promising adsorbents for removing hazardous radionuclides from low-level liquid waste stream especially Cs(I) and Ba(II) radioisotopes.

**Acknowledgment** The author would like to thank the Ministry of Higher Education and Scientific Research of Egyptian government for funding the current work through ParOwn fellowship program and Radiochemistry Laboratory-Chemistry Department of Helsinki University, Finland for hosting the author while conducting part of this research.

## References

1. Malinen LK, Koivula R, Harjula R (2009) Sorption of radiocobalt and its EDTA complex on titanium antimonates. J Hazard Mater 172:875–879
2. Serne RJ, Felmy AR, Cantrell KJ, Krupka KM, Campbell JA, Bolton H, Fredrickson JK (1995) Characterization of radionuclide-chelating agent complexes found in low-level radioactive decontamination waste: literature review. NUREG/CR-6124, US Nuclear Regulatory Commission, Washington, DC, USA
3. Zachara JM, Smith SC, Liua C, McKinley JP, Serne RJ, Gassman PL (2002) Sorption of $Cs^{+}$ to micaceous subsurface sediments from the Hanford site, USA. Geochim Cosmochim Acta 66:193–211
4. Peterson RE, Poston TM (2000) Strontium-90 at the Hanford site and its ecological implications. PNNL-13127. Pacific Northwest National Laboratory, Richland
5. Eccles H (1995) Removal of heavy metals from effluent streams—why select a biological process? Int Biodeterior Biodegrad 35:5–16
6. Roy K, Pal DK, Basu S, Nayak D, Lahiri S (2002) Synthesis of a new ion exchanger, zirconium vanadate, and its application to the separation of barium and cesium radionuclides at tracer levels. Appl Radiat Isot 57:471–474
7. Guan W, Pan J, Ou H, Wang X, Zou X, Hua W, Li C, Wu X (2011) Removal of strontium(II) ions by potassium tetratitanate whisker and sodium trititanate whisker from aqueous solution: equilibrium, kinetics and thermodynamics. Chem Eng J 167: 215–222
8. Marinin DV, Brown GN (2000) Studies of sorbent/ion-exchange materials for the removal of radioactive strontium from liquid radioactive waste and high hardness groundwaters. Waste Manag 20:545–553
9. Chavez ML, de Pablo L, Garcia TA (2010) Adsorption of $Ba^{2+}$ by Ca-exchange clinoptilolite tuff and montmorillonite clay. J Hazard Mater 175:216–223
10. Mishra SP, Singh VK (1998) Ion exchangers in radioactive waste management: Part X. Removal of barium ions from aqueous solutions by hydrous bismuth oxide using radiotracer technique. Appl Radiat Isot 49:43–48
11. Celebi O, Uzum C, Shahwan T, Erten HN (2007) A radiotracer study of the adsorption behavior of aqueous $Ba^{2+}$ ions on nanoparticles of zero-valent iron. J Hazard Mater 148:761–767
12. Iucolano F, Caputo D, Colella C (2005) Permanent and safe storage of $Ba^{2+}$ in hardened phillipsite-rich tuff/cement pastes. Appl Clay Sci 28:167–173

13. Bing Li, Liao J, Wu J, Zhang D, Zhao J, Yang Y, Cheng Q, Feng Y, Liu N (2008) Removal of radioactive cesium from solutions by zinc ferrocyanide. Nucl Sci and Tech 19:88–92
14. Zhang C-P, Gua P, Zhao J, Zhang D, Yue Deng (2009) Research on the treatment of liquid waste containing cesium by an adsorption—microfiltration process with potassium zinc hexacyanoferrate. J Hazard Mater 167:1057–1062
15. Bortun AI, Bortun LN, Clearfield A, Trobajo C, García JR (1998) Synthesis and characterization of the layered zirconium arsenate $Zr_2O_3(HAsO_4)\cdot nH_2O$. Mater Res Bull 33:583–590
16. Gustafsson JP (2009) www.lwr.kth.se/English/OurSoftware/vminteq/verhistory.htm
17. Appel C, Ma LQ, Rhue RD, Kennelley E (2003) Point of zero charge determination in soils and minerals via traditional methods and detection of electroacoustic mobility. Geoderma 113:77–93
18. Mondale KD, Carland RM, Aplan FF (1995) The comparative ion exchange capacities of natural sedimentary and synthetic zeolites. Miner Eng 8:535–548
19. Myroslav S, Buszewski B, Terzyk AP, Namieśnik J (2006) Study of the selection mechanism of heavy metal ($Pb^{2+}$, $Cu^{2+}$, $Ni^{2+}$, and $Cd^{2+}$) adsorption on clinoptilolite. J Colloid Interf Sci 304:21–28
20. Wang X-S, Huang J, Hu H-Q, Wang J, Qin Y (2007) Determination of kinetic and equilibrium parameters of the batch adsorption of Ni(II) from aqueous solutions by Na–mordenite. J Hazard Mater 142:468–476
21. Erdem E, Karapinar N, Donat R (2004) The removal of heavy metal cations by natural zeolites. J Colloid Interf Sci 280: 309–314
22. Behrens EA, Clearfield A (1997) Titanium silicates, M3HTi 4O4(SiO4)3·4H2O (M = Na+, K+), with three-dimensional tunnel structures for the selective removal of strontium and cesium from wastewater solutions. Microporous Mater 11:65–75
23. Basha S, Murthy ZVP (2007) Kinetic and equilibrium models for biosorption of Cr(VI) on chemically modified seaweed, *Cystoseira indica*. Process Biochem 42:1521–1529
24. Motsi T, Rowson NA, Simmons MJH (2009) Adsorption of heavy metals from acid mine drainage by natural zeolite. Int J Miner Process 92:42–48
25. Venkatesan KA, Sukumaran V, Antony MP, Srinivasan TG (2009) Studies on the feasibility of using crystalline silicotitanates for the separation of cesium-137 from fast reactor high-level liquid waste. J Radioanal Nucl Chem 280:129–136
26. Ye X, Wu Z, Li W, Liu H, Li Q, Qing B, Guo M, Ge F (2009) Rubidium and cesium ion adsorption by an ammonium molybdophosphate–calcium alginate composite adsorbent. Colloids Surf A Physicochem Eng Aspects 342:76–83
27. Ma B, Oh S, Shin WS, Choi S-J (2011) Removal of $Co^{2+}$, $Sr^{2+}$ and $Cs^{+}$ from aqueous solution by phosphate-modified montmorillonite (PMM). Desalination 276:336–346
28. Borai EH, Harjula R, Malinen L, Paajanen A (2009) Efficient removal of cesium from low-level radioactive liquid waste using natural and impregnated zeolite minerals. J Hazard Mater 172:416–422
29. Krishna MVB, Rao SV, Arunachalam J, Murali MS, Kumar S, Manchanda VK (2004) Removal of $^{137}Cs$ and $^{90}Sr$ from actual low level radioactive waste solutions using moss as a phytosorbent. Sep Purif Technol 38:149–161
30. Ghaemi A, Torab-Mostaedi M, Ghannadi-Maragheh M (2011) Characterizations of strontium(II) and barium(II) adsorption from aqueous solutions using dolomite powder. J Hazard Mater 190:916–921
31. Khanchi AR, Yavari R, Pourazarsa SK (2007) Preparation and evaluation of composite ion-exchanger for the removal of cesium and strontium radioisotopes. J Radioanal Nucl Chem 273: 141–145
32. Ma B, Shin WS, Oh S, Park YJ, Choi SJ (2010) Adsorptive removal of Co and Sr ions from aqueous solution by synthetic hydroxyapatite nanoparticles. Sep Sci Technol 45:453–462
33. Chmielewska-Horvathova E, Lesng J (1995) Study of sorption equilibria in the systems: water solutions of inorganic ions–clinoptilolite. J Radioanal Nucl Chem Lett 201:293–301
34. Singhal RK, Basu H, Manisha V, Reddy AVR, Mukherjee T (2011) Removal of low level americium-241 from potable water originated from different geochemical environments by calcium alginate. Desalination 280:313–318
35. Matsumura T, Usuda S (1998) Applicability of insoluble tannin to treatment of waste containing americium. J Alloys Compd 271–273:244–247